

6

Quantum billiards, random matrices and mesoscopic systems.

6.1 Billiards.

An important class of non integrable classical systems are *billiard systems*. In a billiard a particle moves freely in two dimensions until it encounters a boundary in which case it undergoes a perfectly elastic collision. These systems are often *ergodic* which means that all orbits eventually pass through almost every point of the surface of constant energy, $H(p, q) = E$ (a $2N - 1$ dimensional surface in general), instead of being confined to an N -torus like integrable systems. Ergodicity is usually associated with chaotic motion (but is not equivalent to it), where we define chaotic motion in terms of sensitive dependence on initial conditions, (eg in terms of a Bernoulli map).

Sinai showed that for two degrees of freedom the billiard motion of a particle moving on a two-dimensional square with periodic boundary conditions which contains a perfectly reflecting obstacle of radius R is both ergodic and chaotic. See figure 6.1. Another example is the Bunimovich stadium consisting of two semi circles with radius R joined by parallel straight lines of length L . see figure 6.1. In these systems a typical orbit passes through every point, with almost every direction, if we take a long enough time. However there are special, isolated, orbits that are perfectly regular

6.2 Mesoscopic system.

Modern fabrication technology has advanced to the stage where it is possible to fabricate confining potentials for electrons that constitute small cavities for de Broglie waves. Such devices are often called quantum dots as the electron is confined in all three spatial dimensions. In GaAs devices these cavities are made by first confining electrons to a thin layer, called

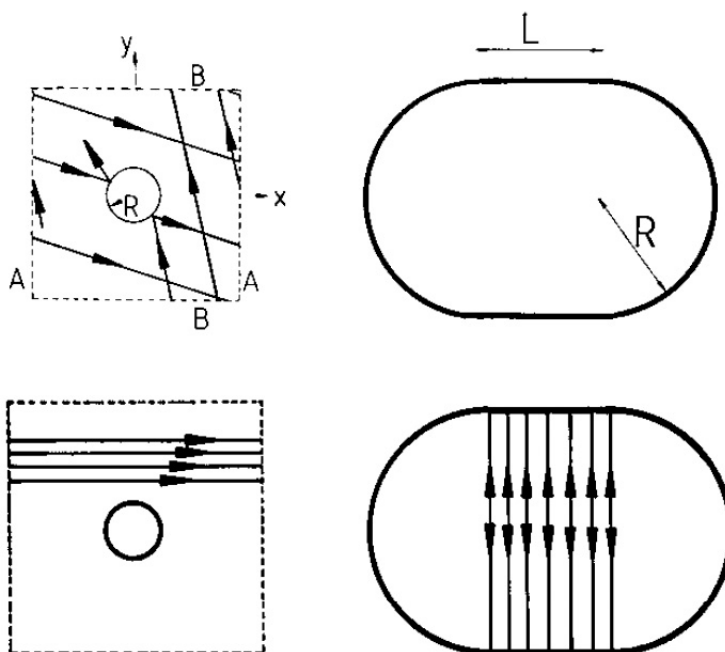


Fig. 6.1. The Sinai billiard (left) and the Bunimovich stadium (right). below are shown isolated regular orbits. [From M Berry Les Houches notes]

a two dimensional electron gas (2DEG), between a crystal of GaAs and a crystal of AlGaAs. Then a surface gate is used to deplete electrons in the 2DEG in a way that reflects the geometry of the surface gate (see figure 6.2). An alternative way to fabricate a quantum dot is to use a very small metallic grain. In such devices the standard laws of electronics, such as Ohms law, no longer hold. A small conductor shows Ohmic behaviour when its dimensions are much larger than three crucial length scales;

- the de Broglie wavelength as determined by the kinetic energy of the electron,
- the mean free path, the distance an electron travels before its initial momentum is destroyed by scattering,
- the phase relaxation length, the distance an electron travels before the corresponding de Broglie wave suffers a random phase shift.

In typical semiconductor devices at low temperature (below 4K) the mean free path and phase relaxation length are comparable between 10 and 100 microns. The mean free path in polycrystalline metal films can be as small as 50nm. In semiconductors the de Broglie wavelength is between 10 nm and 100nm. In metals the de Broglie wavelength is of the order of the distance between atoms, 0.1nm to 1nm.

In both semiconductors and metals the systems must be held at very low temperature to ensure that the motion of an extra electron injected, with a definite momentum, into the device is *ballistic*. This also requires low bias voltages so that the energy of the injected electron is not too large. This means that the plane wave corresponding to this injected electron propagates without inelastic scattering and this can happen at low temperatures in very pure materials. In reality of course this is not strictly true and the electron will scatter off an impurity or another electron excited above the zero temperature Fermi level. The average distance a ballistic electron travels before scattering is called the phase coherence length L_ϕ . It can be thought of as the distance the plane wave propagates before its phase undergoes a random shift. At temperatures of around 50mk in GaAs/AlGaAs heterostructures this length is typically 30-40 μ m. This is usually bigger than the size of the confining region.

A ballistic electron injected into the confining region behaves like a free particle until it bounces elastically off the confining potential. When working at very low temperatures, the Fermi energy is much greater than the thermal excitation energy, $k_B T$. In that case it is no longer appropriate to view the current as due to a slow drift of carriers in a Fermi gas, but rather the current is carried by a few electrons close to the Fermi energy which move much faster. Thus conductance in such *degenerate*

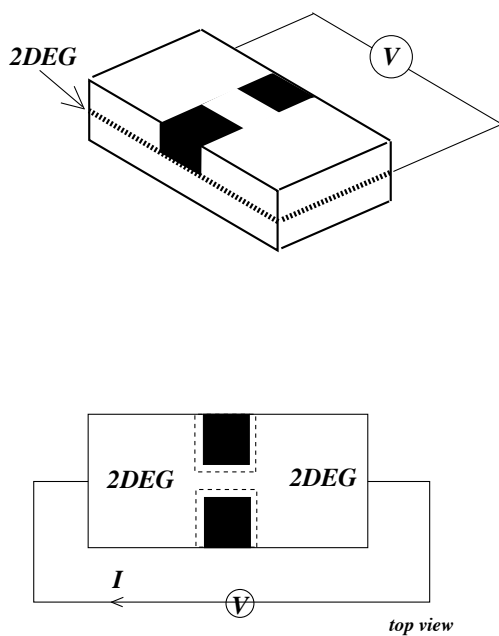


Fig. 6.2. Schematic indication of confined two dimensional electronic system using 2DEG heterostructure and surface gates.

conductors is determined by the properties of electrons near the Fermi energy rather than the entire sea of electrons. If the confining region is two dimensional, the system is very much like a Hamiltonian billiard system. This is the case we will consider in some depth. On the other hand, the electron is a very quantum mechanical object and if it is in a state of definite momentum then we should describe it quantum mechanically as a plane wave. We are thus faced with the necessity of finding a quantum description of Hamiltonian billiards if we are to describe such a mesoscopic system. As we shall see, a knowledge of the corresponding classical system provides a path to understanding the quantum scattering of an electron in a mesoscopic system. As much of the future of semiconductor technology will be based on such devices, this is an important problem.

For further information on mesoscopic systems see;

- *Quantum Technology*, G.J.Milburn, Allen and Unwin, (1996)
- *The Quantum Dot*, R. Turton, Freeman, (1995).
- *Electronic Transport in Mesoscopic systems*, S. Datta, Cambridge University Press, (1997).

6.3 Prelude to quantum scattering

Consider a one dimensional potential of the form,

$$V(x) = \begin{cases} \infty & x \leq 0 \\ 0 & 0 < x < a \\ V_0 & a \leq x \leq b \\ 0 & x > b \end{cases} \quad (6.1)$$

Let $u_{\pm}(x)$ be the position probability amplitude for particles traveling in the $\pm x$ direction, in the region $x > b$, with definite energy $E < V_0$. These are plane wave states of the form

$$u_{\pm}(x) = e^{\pm ikx} \quad (6.2)$$

where $k^2 = \frac{2mE}{\hbar^2}$. By matching the boundary condition it is easy to show that at $x = b$,

$$\frac{u_+(b)}{u_-(b)} = -e^{2i\phi(k)} \quad (6.3)$$

where

$$\tan \phi(k) = \frac{k [f(k)e^{\alpha(b-a)} + e^{-\alpha(b-a)}]}{\alpha [f(k)e^{\alpha(b-a)} - e^{-\alpha(b-a)}]} \quad (6.4)$$

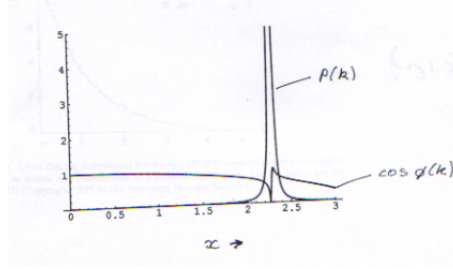


Fig. 6.3. The relative occupation probability for the bound state versus the input energy with $w = 3, l = 1.0$

where

$$\alpha = \sqrt{\frac{2m(V_0 - E)}{\hbar^2}} \quad (6.5)$$

$$f(k) = \frac{\alpha \tan ka + k}{\alpha \tan ka - k} \quad (6.6)$$

There is only a phase shift between left-going and right-going states.

We can calculate the (relative) probability $P(k)$ to find the particle in $0 \leq x \leq a$, relative to the probability to find a particle at $x > b$ with negative momentum,

$$P(k) = 4 \left\{ \sin \phi(k) \cosh(\alpha(b - a)) - \frac{k}{\alpha} \cos \phi(k) \sinh(\alpha(b - a)) \right\}^2 \quad (6.7)$$

We now define the dimensionless parameters, the scaled energy x , the scaled barrier strength w and the scaled barrier length l ,

$$x = ka \quad (6.8)$$

$$w^2 = \frac{2mV_0}{\hbar^2}(b - a) \quad (6.9)$$

$$l^2 = \frac{b}{a} - 1 \quad (6.10)$$

In figure 6.3 we plot the function $P(k)$ and $\cos \phi(k)$ versus the scaled input energy, x . This is a kind of spectrum of excitation for the quasi bound state in the well. Note the *resonance* at a particular value of input energy. Why does this maximum occur?

In a classical description of this system, if the energy of the particle is $E < V_0$ it cannot penetrate the barrier and there are two regions of motion one bounded, inside the well and the other unbounded outside the

well. The bounded motion is periodic with period T given by the time taken to traverse the well from $x = 0$ to $x = a$ and back again. At the boundaries the collisions are elastic so energy is conserved. The period is easily seen to be given by

$$T(E) = a\sqrt{\frac{2m}{E}} \quad (6.11)$$

As the period (and frequency) depend on energy this is a nonlinear oscillator. It is obviously non harmonic. The nonlinear frequency can also be obtained by computing the action $J(E)$ on a periodic orbit. The action of an orbit is defined as the phase space area bounded by the orbit divided by 2π . Thus

$$J(E) = \frac{a}{\pi}\sqrt{2mE} \quad (6.12)$$

from which the nonlinear frequency is given by $\omega(E) = (dJ/dE)^{-1}$ which gives the same result for the period as Eq.(6.11).

We can now use the semiclassical quantisation rules to estimate the allowed energy levels for the equivalent problem. Recall that the rule says we are only allowed those orbits for which the phase space area divided by \hbar , and adjusted for the Maslov index, is an integer multiple of 2π . For billiard problems the Maslov index correction is not the same as the case of a soft potential. In fact each reflection leads to a phase change of π rather than $\pi/4$. There are two turning points in this case. The semiclassical quantisation condition then becomes

$$2L\sqrt{2mE_n} - 2\pi = 2\pi n \quad n = 0, 1, 2, \dots \quad (6.13)$$

from which we find the allowed energies are

$$E_n = \frac{\pi^2 \hbar^2 n^2}{2ma^2} \quad n = 1, 2, \dots \quad (6.14)$$

This is the spectrum of energies for the states of the infinite square well.

If we now return to the excitation spectrum in Eq.(6.7) it is easy to show that in the limit of $E \ll V_0$ the peak of the spectrum corresponds to the allowed energies of the bound state of the infinite square well. We can now draw together some lessons. The infinite square well is a very simple kind of one dimensional billiard. The allowed energies of which can be found by finding the classical periodic orbits and then applying the semiclassical quantisation rules, which in this case work exactly. If we now weaken one boundary so that we can probe the allowed energies by scattering particles of fixed energy we can excite the allowed bound states in the well which correspond to a rapid phase change of the scattered quantum probability amplitude. However the very act of weakening the potential in order to

probe necessarily shifts the resonances slightly from the infinite square well result. However we can try and make this disturbance as small as possible.

This example serves to illustrate our approach to the problem of two dimensional billiard systems. As for this one dimensional billiard, we will approach the physics of the system as a kind of scattering problem. The classical dynamics of the corresponding closed system will determine, to a good approximation, what we see in the quantum scattering problem. However we need to keep in mind that to probe a billiard spectroscopically we need to weaken the classical perfect billiard system to some extent. We need to keep the disturbance due to this measurement to a minimum. Given this, we seek to understand the quantum scattering problem by determining the classical billiard problem first. The key question however is how well the semiclassical intuition can work for a chaotic billiard problem.

6.4 Quantum billiards and microwave cavities.

In a two dimensional billiard system a particle of mass m moves freely in the plane until it encounters a wall, at which point it undergoes a perfectly elastic collision. The quantum description of this problem is in terms of the Schrödinger equation in the coordinate representation

$$i\hbar \frac{\partial \psi(x, y, t)}{\partial t} = -\frac{\hbar^2}{2m} \nabla^2 \psi(x, y, t) \quad (6.15)$$

subject to the *Dirichlet* boundary condition

$$\psi(x, y, t)|_S = 0 \quad (6.16)$$

where S denotes the curve that defines the boundary of the billiard. The energy eigenstates $\psi_n(x, y)$ and allowed energies, $E_n = \hbar\omega_n$, are obtained by separating the time dependence as

$$\psi_n(x, y, t) = \psi_n(x, y) e^{-i\omega_n t} \quad (6.17)$$

and solving the time independent equation

$$-\frac{\hbar^2}{2m} \nabla^2 \psi_n(x, y) = E_n \psi_n(x, y) \quad (6.18)$$

$$\nabla^2 \psi_n(x, y) + k_n^2 \psi_n(x, y) = 0 \quad (6.19)$$

with the dispersion relation

$$\omega_n = \frac{\hbar}{2m} k_n^2, \quad (6.20)$$

subject to the same boundary condition Eq.(6.16).

There is a very similar system of equations for the case of an electromagnetic wave sustained inside a conducting boundary; a resonant cavity. The equation for the electric and magnetic field amplitudes are

$$(\nabla^2 + k^2)\vec{E} = 0 \quad (6.21)$$

$$(\nabla^2 + k^2)\vec{B} = 0 \quad (6.22)$$

with the dispersion relation $\omega = ck$ and the boundary conditions

$$\vec{n} \times \vec{E} = 0 \quad (6.23)$$

$$\vec{n} \cdot \vec{B} = 0 \quad (6.24)$$

where \vec{n} is a unit normal to the surface of the boundary. To make this look like a quantum billiard problem we consider resonators with cylindrical symmetry, but varying cross sections. Taking the z axis parallel to the axis of cylindrical symmetry the boundary conditions are

$$E_z|_S = 0 \quad (6.25)$$

$$\vec{\nabla}_\perp B_z|_S = 0, \quad (6.26)$$

where $\vec{\nabla}_\perp$ denotes the normal derivative. These can be satisfied for transverse magnetic modes (TM)

$$E_z(x, y, z) = E(x, y) \cos(n\pi z/d) \quad (6.27)$$

$$B_z(x, y, z) = 0 \quad (6.28)$$

where

$$\left[\nabla^2 + k^2 - \left(\frac{n\pi}{d} \right)^2 \right] E = 0 \quad (6.29)$$

with Dirichelet boundary condition $E(x, y)|_S = 0$ on the surface. For frequencies $\nu < c/2d$ ($k < \pi/d$) only TM modes with $n = 0$ are possible. Thus the electric field in the x, y plane must satisfy $(\nabla^2 + k^2)E = 0$ with Dirichelet boundary conditions. The dispersion relation for electromagnetic waves however is different ($\omega = ck$). The equivalence to the quantum billiard problem is apparent. For this reason many early experiments on quantum billiards were in fact microwave cavity experiments. However it is worth stressing the crucial difference between the quantum and microwave case. In the microwave case we are concerned with a true field amplitude in the cavity. In the quantum case the analogous object is a *probability amplitude*. This means the kinds of measurements that we could consider in the two cases are very different. It is possible to measure a field amplitude, while generally we cannot measure a quantum probability amplitude directly (for that matter we cannot measure

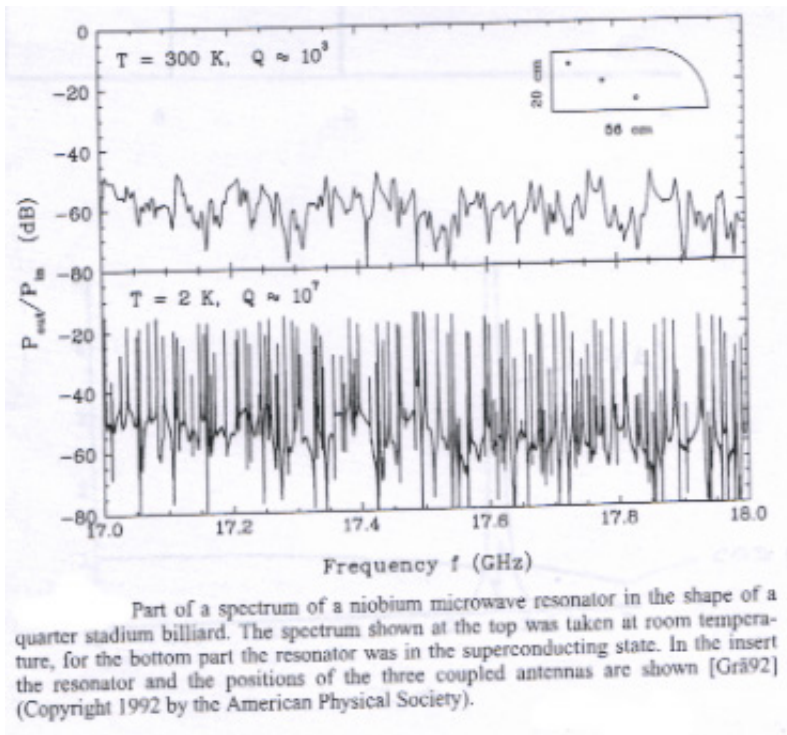


Fig. 6.4. From 2.12 in Stockman. The spectra at two different temperatures are recorded. At room temperature there is a significant amount of thermally excited background radiation that masks the cavity spectrum. At low temperature with the walls are superconducting, and the spectra reflects more closely the billiard spectrum.

a probability directly either!). Rather we measure some other quantity, such as position of an electron, the statistics of which measurements are determined by the quantum probability amplitude.

In the microwave cavity experiments we need to find a way to measure the field inside the cavity. This requires that we open the cavity up in some way, so the cavity walls are no longer perfectly reflecting. This is usually done by introducing a small antenna into the resonator through a small hole, and measuring the amount of power reflected back when the antenna is used to excite the cavity. An example is shown in figure 6.4. The reflected power is monitored as a function of the frequency of the injected signal to give a spectrum. Each minimum in the reflected power corresponds to a resonant eigenfrequency of the cavity.

The spectrum in Figure 6.4 looks very complex, which we will see reflects the corresponding complex chaotic trajectories of the correspond-

ing billiard problem. Many decades ago similar complex spectra turned up in nuclear physics. An approach to analysis was adopted based on eigenvalue spacing distributions. The sequence of successive eigenvalue differences $s_n = E_n - E_{n-1}$ is computed and the relative frequency of values of s_n plotted to construct a distribution $P(s)$ of eigenvalue spacings. The variable s_n is scaled so that the average spacing is unity. It was found that these distributions could be classified into a few general classes that reflected fundamental dynamical properties of the system. In particular it was found that eigenvalues either tended to bunch so that $P(s)$ was peaked at zero or they seemed to repel each other so that $P(s)$ is peaked away from zero. In the case of the stadium billiard the spacing distribution is well fitted by the Wigner distribution

$$P(s) = \frac{\pi}{2} s \exp\left[-\frac{\pi}{4} s^2\right] \quad (6.30)$$

It is no coincidence that this distribution is associated with a billiard problem that is chaotic. Indeed if we measure the spectrum of a rectangular cavity, for which the corresponding billiard problem is integrable, we find that

$$P(s) = e^{-s} \quad (6.31)$$

a Poisson distribution which exhibits level bunching.

In the case of nuclear spectra the conjecture was made that the spacing distributions could be understood if the corresponding Hamiltonians were drawn from an ensemble of random matrices. This work was largely pioneered by Wigner, Dyson and Mehta. In 1984 however Bohigas, Gianconi and Schmidt conjectured that random matrix theory could be used to describe the statistical level spacing of quantum systems which were classically chaotic. The BGS conjecture says that:

“statistical properties of long sequences of energy levels of generic quantum systems whose classical counterparts are chaotic have their pattern in long sequences of eigenvalues of large random Hermitian matrices with independent, identically distributed entries.”

This has subsequently been vindicated in countless real and numerical experiments. Yet curiously a rigorous proof is elusive.

6.5 Random matrices.

A hamiltonian for a complex system may exhibit certain symmetries, for example it may be invariant under rotations. In quantum mechanics this means that the hamiltonian is invariant under a unitary transformation representing an element of the symmetry group. The generator of the

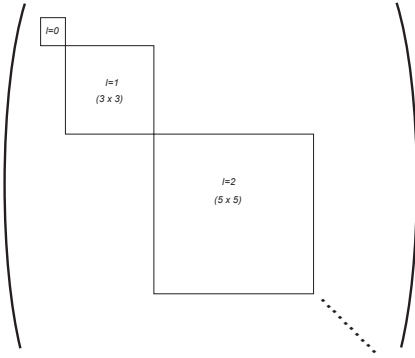


Fig. 6.5. The scheme of a Hamiltonian matrix in block diagonal form. All matrix elements outside the squares are zero.

transformation will then commute with the Hamiltonian which implies that it is a constant of the motion. Thus if the system starts in an eigenstate of the generator it remains in an eigenstate of the generator. Another consequence of the commutation of the generator and the Hamiltonian is that both operators may be simultaneously diagonalised. Consider the case of the hydrogen atom. The central Coulomb potential is invariant under arbitrary rotations which are represented by a unitary operator of the form $U(\vec{n}, \theta) = \exp(-i\theta \vec{L} \cdot \vec{n})$ where \vec{n} is a unit vector while θ represents the angle of rotation around the direction \vec{n} . The operator valued vector $\vec{L} = \hat{L}_x \vec{x} + \hat{L}_y \vec{y} + \hat{L}_z \vec{z}$ is the operator for angular momentum. The eigenvalues of total angular momentum squared, $\hat{L}^2 = \hat{L}_x^2 + \hat{L}_y^2 + \hat{L}_z^2$ are $\hbar^2 l(l+1)$ $l = 0, 1, 2, \dots$. The Hamiltonian may then be represented in block diagonal form where each block corresponds to a fixed value of l , see figure 6.5

In the case of the hydrogen atom there are extra symmetries which permit us to completely diagonalise the hamiltonian in terms of three quantum numbers n, l, m corresponding to conservation of total energy, total angular momentum and one component of angular momentum. As the number of constants of the motion is equal to the number of degrees of freedom the system is totally integrable.

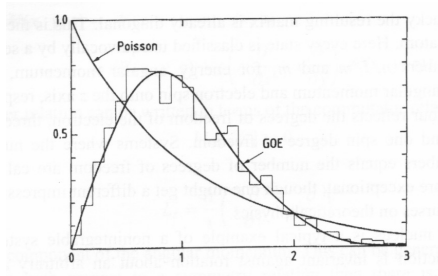


Fig. 6.6. The nearest neighbour spacing distribution for the nuclear data ensemble. It contains 1726 energy levels of 36 sequences of 32 nuclei. The distribution peaked away from $s = 0$ is the Wigner distribution also known as the gaussian orthogonal ensemble (from Stöckman fig 3.1)

However this is the exception rather than the rule and in general we will only be able to block diagonalise the Hamiltonian with each block corresponding to some reduced set of conserved quantities for subspaces that remain invariant under the corresponding symmetry transformation. This is precisely the situation for nuclear physics where the only symmetries are angular momentum and parity. However for nuclei with many nucleons the number of degrees of freedom is very large and the systems are non integrable.

When we make a statistical analysis of the spectrum of a hamiltonian we must first block diagonalise the matrix and compare eigenvalues only within a block corresponding to one of the eigenvalues of the conserved quantity: this is called subspectra. Determining the symmetries of a complex Hamiltonian is the first step.

The next step requires that we rescale the energies so that the average density of states is unity. Then various statistics may be calculated, for example the nearest neighbour spacing distribution $p(s)$. Bohigas and co workers have compiled a large number of energy levels for complex nuclei known as the *nuclear data ensemble*. In figure 6.6 is shown the spacing distribution for combining the results of 30 different subspectra.

In figure 6.6 the Poisson distribution is also shown. This corresponds to the spectra of fully integrable systems. In such systems the hamiltonian is completely diagonalised and each eigenvalue makes up a symmetry class of its own. It is thus reasonable to assume the eigenvalues are completely uncorrelated. Let the probability to find an eigenvalue between E and $E + dE$ be a constant which we take as unity after rescaling the average energy eigenvalue spacing. Let us now calculate the probability, $p(s)$, that

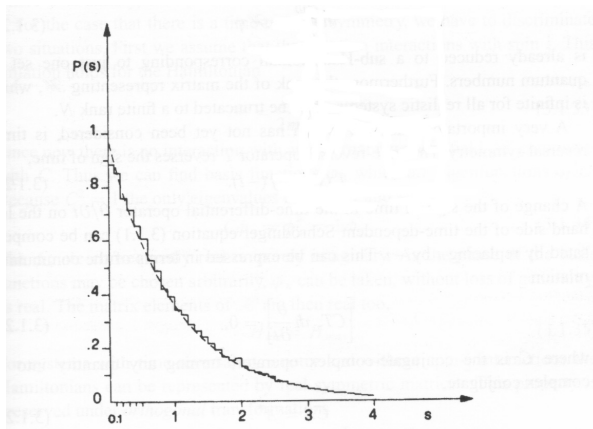


Fig. 6.7. level spacing distribution for the first 100,000 eigenvalues of a rectangular billiard (figure 3.3 Stöckman)

from a given eigenvalue, we will find only one other a distance s away, with no other eigenvalues between. If we divide up the interval of length s into N equally spaced intervals, the probability is easily calculated as

$$p(s)ds = N \xrightarrow{\text{lim}} \infty \left(1 - \frac{s}{N}\right)^N ds \quad (6.32)$$

In the limit this is $p(s) = e^{-s}$.

In figure 6.7 is shown the eigenvalue distribution for a rectangular billiard with side length a, b , with $a/b = \sqrt{\pi/3}$, irrational. The eigenvalues are easily given by

$$E_n = \frac{\hbar^2}{2m} \left[\left(\frac{\pi n}{a}\right)^2 + \left(\frac{\pi m}{b}\right)^2 \right], \quad n, m = 0, 1, 2, \dots \quad (6.33)$$

To define a random matrix, H , we simply imagine that in an arbitrary basis the matrix elements are random numbers with some form of distribution, for example gaussian. However we must ensure that the matrix is indeed a valid hamiltonian, which is to say it is Hermitian $H^\dagger = H$. In the eigenbasis every Hamiltonian is real. However we are at liberty to use any basis which is a unitary transformation of the eigenbasis. In general this will result in a complex hermitian matrix. We can classify hermitian matrices into classes according to how they transform under different classes of unitary transformations.

If the Hamiltonian is not time reversal invariant (eg it contains a magnetic field), then the most we can require is that the hermiticity property

is preserved. The ensemble of such random matrices is then called the *random unitary ensemble*.

If the Hamiltonian is invariant under time reversal and does not contain spin half interactions, it can always be chosen as real (see Stöckmann, chapter 3, for a full discussion). This property is preserved under orthogonal transformations.

$$H' = OHO^T \quad OO^T = 1 \quad (6.34)$$

In that case we must restrict the class of unitary transformations to be simply orthogonal matrices, and we will refer to the ensemble of random matrices with this property as an *orthogonal ensemble*.

Consider systems with time reversal invariance and with spin interactions. A typical example is the spin-orbit interaction

$$H = g\vec{L} \cdot \vec{S} \quad (6.35)$$

where

$$\vec{L} = -i\hbar\vec{r} \times \vec{p} \quad (6.36)$$

is orbital angular momentum and $\vec{S} = \frac{\hbar}{2}\vec{\sigma}$ is the spin of the particle and $\vec{\sigma} = \sigma_x\vec{x} + \sigma_y\vec{y} + \sigma_z\vec{z}$ and σ_α are the Pauli matrices.

It turns out that all such Hamiltonians are even dimensional and transform into each other under the *symplectic* transformation:

$$H' = SHS^R \quad (6.37)$$

where S is a symplectic matrix which means it must satisfy $SS^R = 1$ with

$$S^R = ZS^T Z^{-1} = -ZSZ \quad (6.38)$$

where Z is in block diagonal form

$$Z_{nm} = i\delta_{nm}\sigma_y \quad (6.39)$$

where σ_y is the Pauli matrix

$$\sigma_y = \begin{pmatrix} 0 & -i \\ i & 0 \end{pmatrix} \quad (6.40)$$

We will only consider in detail the case of the orthogonal ensemble with gaussian distributions. We are thus led to the gaussian orthogonal ensemble or GOE. The other two symmetry classes with gaussian statistics are called the gaussian unitary ensemble (GUE) and the gaussian symplectic ensemble (GSE).

A real symmetric matrix in N dimensions requires $N(N+1)/2$ real numbers to specify the matrix elements. The joint probability distribution

$p(H_{11}, H_{12}, \dots, H_{NN})$ is then invariant under orthogonal transformations $p(H_{11}, H_{12}, \dots, H_{NN}) = p(H'_{11}, H'_{12}, \dots, H'_{NN})$. Now the trace of any matrix is invariant under orthogonal transformation $\text{tr}(OAO^T) = \text{tr}(A)$. This means that the joint distribution must be a function of the trace of powers of the Hamiltonian;

$$p(H_{11}, H_{12}, \dots, H_{NN}) = f[\text{tr}H, \text{tr}(H^2), \dots] \quad (6.41)$$

If we now require the matrix elements to be uncorrelated

$$p(H_{11}, H_{12}, \dots, H_{NN}) = p(H_{11})p(H_{12}) \dots p(H_{NN}) \quad (6.42)$$

the only way to satisfy both Eqs.(6.41,6.42) is if

$$p(H_{11}, H_{12}, \dots, H_{NN}) = C \exp [-B\text{tr}(H) - A\text{tr}(H^2)] \quad (6.43)$$

As this is Gaussian in form, we can shift the average to ensure that $B = 0$. The normalisation fixes the factor C ,

$$\int p(H_{11}, H_{12}, \dots, H_{NN}) dH_{11} \dots dH_{NN} = 1 \quad (6.44)$$

We are thus led to the distribution

$$p(H_{11}, H_{12}, \dots, H_{NN}) = \left(\frac{A}{\pi}\right)^{N/2} \left(\frac{2A}{\pi}\right)^{N(N-1)/2} \exp\left(-A \sum_{n,m} H_{nm}^2\right) \quad (6.45)$$

We now turn to the eigenvalue distribution. The hamiltonian may be diagonalised by an orthogonal transformation $H_{nm} = \sum_k O_{nk} E_k O_{mk}$. It would appear that we need to know the actual $N(N-1)/2$ matrix elements, p_α , which diagonalises the hamiltonian. However if we use the fact that the trace is the same in any basis,

$$\sum_{n,m} H_{nm}^2 = \sum_k E_k^2 \quad (6.46)$$

we can write the new probability distribution in terms of the new variables E_k as

$$p(H_{11}, H_{12}, \dots, H_{NN}) dH_{nm} \sim \exp\left(-A \sum_k E_k^2\right) |J| dE_k dp_\alpha \quad (6.47)$$

where J is the Jacobian of the transformation

$$|J| = \left| \frac{\partial(H_{NM})}{\partial(E_k, p_\alpha)} \right| \quad (6.48)$$

It can be show that the determinant of J can be written as

$$|J| = g(p_\alpha) \prod_{i>j} (E_i - E_j) \quad (6.49)$$

where $g(p_\alpha)$ is a function of the diagonalising matrix alone. After integrating over the variables p_α we find

$$P(E_1, E_2, \dots, E_N) \sim \prod_{n>m} (E_n - E_m) \exp \left(-A \sum_n E_n^2 \right) \quad (6.50)$$

As an example we consider the case of real symmetric 2×2 matrices

$$H = \begin{pmatrix} H_{11} & H_{12} \\ H_{21} & H_{22} \end{pmatrix} \quad (6.51)$$

The eigenvalues are given by

$$E_{\pm} = \frac{1}{2}(H_{11} + H_{22}) \pm \frac{1}{2} [(H_{11} - H_{22})^2 + 4H_{12}^2]^{1/2} \quad (6.52)$$

The orthogonal transformation that achieves this diagonalisation depends on a single parameter θ so that

$$\begin{aligned} H_{11} &= E_+ \cos^2 \theta + E_- \sin^2 \theta \\ H_{22} &= E_+ \sin^2 \theta + E_- \cos^2 \theta \\ H_{12} &= (E_+ - E_-) \cos \theta \sin \theta \end{aligned}$$

The Jacobian is then

$$J = \det \frac{\partial(H_{11}, H_{22}, H_{12})}{\partial(E_+, E_-, \theta)} = E_+ - E_- \quad (6.53)$$

Thus $P(E_+, E_-) = C|E_+ - E_-|e^{-A(E_+^2 + E_-^2)}$.

The nearest neighbour spacing distribution is now easily calculated. We will only consider the 2×2 case as the results are independent of the dimension.

$$p(s) = \int_{-\infty}^{\infty} dE_1 \int_{-\infty}^{\infty} dE_2 P(E_1, E_2) \delta(s - |E_1 - E_2|) \quad (6.54)$$

$$= C \int_{-\infty}^{\infty} dE_1 \int_{-\infty}^{\infty} dE_2 |E_1 - E_2| \exp \left(-A \sum_n E_n^2 \right) \quad (6.55)$$

$$\times \delta(s - |E_1 - E_2|) \quad (6.56)$$

the two constants are fixed by

$$\int_0^\infty p(s) ds = 1 \quad (6.57)$$

$$\int_0^\infty sp(s) ds = 1 \quad (6.58)$$

Thus

$$p(s) = \frac{\pi}{2} s \exp\left(-\frac{\pi}{4} s^2\right) \quad (6.59)$$

For completeness we give the eigenvalue spacing distributions for the GUE and the GSE as well as the GOE.

$$p(s) = \begin{cases} \frac{\pi}{2} s \exp\left(-\frac{\pi}{4} s^2\right) & \text{(GOE)} \\ \frac{32}{\pi^2} s^2 \exp\left(-\frac{4}{\pi} s^2\right) & \text{(GUE)} \\ \frac{2^{18}}{3^6 \pi^3} s^4 \exp\left(-\frac{\pi}{4} s^2\right) & \text{(GSE)} \end{cases} \quad (6.60)$$

Note the dependence at small spacing. The GOE is linear, the GUE is quadratic and the GSE is quartic. In the case of Floquet operators we need to consider *Gaussian circular ensembles* as all eigenvalues lie on the unit circle. There is an equivalent breakdown in terms of orthogonal, unitary and symplectic transformations.

An important function of the spectrum of a quantum system is the *density of states* defined as

$$\rho(E) = \sum_n \delta(E - E_n) \quad (6.61)$$

This is a standard way to capture the spectrum of a quantum mechanical system. In many cases it has been found that we can write the density of states as the sum of a smooth part, called the average density of states and a quasiperiodic oscillating part,

$$\rho(E) = \overline{\rho(E)} + \rho_{osc}(E) \quad (6.62)$$

The average here is a spectral average taken over the energy eigenvalues. However it can be shown that this can often be replaced to a good approximation by an average over some ensemble of random matrices provided that the number of levels is very large. This is a kind of ergodic theorem for energy eigenvalues and underpins the BGS conjecture. A great deal of mathematical effort has gone into characterising the oscillatory part of the density of states. Gutzwiller demonstrated a semiclassical method to calculate $\rho_{osc}(E)$ based on an understanding of the periodic orbits of the corresponding classical system. We will return to this later. For now we concentrate on the average density of states for the random matrix ensemble.

What is the average density of states, averaged over the complete ensemble of random matrices? Before doing this however we describe a way to represent the density of states as a *trace formula*. We begin by representing the delta function as the limit of a Lorentzian curve of zero width

$$\delta(E) = \lim_{\epsilon \rightarrow 0} \frac{\epsilon}{\pi} \frac{1}{\epsilon^2 + E^2} \quad (6.63)$$

Exercise 6.1 Show that this is indeed a representation of the delta function, that is, show that

$$\lim_{\epsilon \rightarrow 0} \int dE f(E - E_0) \frac{\epsilon}{\pi} \frac{1}{\epsilon^2 + E^2} = f(E_0) \quad (6.64)$$

Thus

$$\rho(E) = \lim_{\epsilon \rightarrow 0} \frac{\epsilon}{\pi} \sum_n \frac{1}{\epsilon^2 + (E - E_n)^2} \quad (6.65)$$

$$= - \lim_{\epsilon \rightarrow 0} \frac{1}{\pi} \text{Im} \sum_n \frac{1}{E - E_n + i\epsilon} \quad (6.66)$$

Now we can use

$$\sum_n \frac{1}{E - E_n} = \text{tr} \left(\frac{1}{E - H} \right) \quad (6.67)$$

so that

$$\rho(E) = - \frac{1}{\pi} \text{Im} \left(\text{tr} \left(\frac{1}{E - H} \right) \right) \quad (6.68)$$

where the $i\epsilon$ term is not written explicitly to simplify notation but must be inserted. The average density of states may thus be calculated by

$$\mathcal{E}(\rho(E)) = - \frac{1}{\pi} \text{Im} S \quad (6.69)$$

where

$$S = \mathcal{E} \left(\text{tr} \left(\frac{1}{E - H} \right) \right) \quad (6.70)$$

$$= \sum_{n=0}^{\infty} \frac{1}{E^{n+1}} \mathcal{E}(\text{tr} H^n) \quad (6.71)$$

where the series converges if E exceeds all the eigenvalues of H in magnitude, and we assume implicitly that $E \rightarrow E + i\epsilon$.

The explicit calculation of the average over the gaussian distributions is tedious. Let us take the dimension of \hat{H} is N . The result is

$$\mathcal{E}(\rho(E)) = \begin{cases} \frac{A}{\pi} \sqrt{\frac{2N}{A} - E^2} & |E| < \frac{\sqrt{2N}}{A} \\ 0 & |E| > \frac{\sqrt{2N}}{A} \end{cases} \quad (6.72)$$

It is usual to write to choose

$$A = \frac{\pi^2}{2N} \quad (6.73)$$

we get the *Wigner semicircle law*,

$$\mathcal{E}(\rho(E)) = \begin{cases} \sqrt{1 - \left(\frac{\pi E}{2N}\right)^2} & |E| < \frac{2N}{\pi} \\ 0 & |E| > \frac{2N}{\pi} \end{cases} \quad (6.74)$$

For energies $|E| \ll N$ the density of states is constant. We usually only consider this limit. As the Hamiltonians of real chaotic systems have infinite dimension this is a reasonable thing to do.

There is another way to write the density of states as a trace formula. Using the Fourier representation of a delta function we can write

$$\rho(E) = \sum \int_{-\infty}^{\infty} dt e^{it(E-E_n)} \quad (6.75)$$

$$= \int_{-\infty}^{\infty} dt \mathcal{P}(t) e^{iEt} \quad (6.76)$$

where

$$\mathcal{P}(t) = \sum_n e^{-iE_n t} \quad (6.77)$$

$$= \text{tr}(U(t)) \quad (6.78)$$

In other words the density of states is the Fourier transform of the trace of the unitary evolution operator for the dynamical system.

6.6 Mesoscopic electronics

We now consider the scattering of electrons from mesoscopic billiard systems as described in the introduction. The mesoscopic cavity is connected to leads which act as waveguides for the de Broglie waves of electrons. The leads are connected to reservoirs maintained at local equilibrium by an external voltage. The measured quantity is the *conductance* G of the total device. The objective is to understand the conductance through the elastic scattering of an electron in the mesoscopic cavity. The multiple scattering of the electron wave reflected from the cavity walls that gives rise to complex interference effects and ensures the conductance has a strong dependence on the energy of the injected electrons (which is essentially the Fermi energy ϵ_f of the reservoir connected to this lead) as well as the geometry of the cavity. If an external magnetic field is present additional interference effects can arise due to the Aharonov-Bohm effect

in which electron paths that enclose magnetic flux can acquire additional phase shifts. The changing interference causes the conductance to change. The sensitive dependence of G on small changes in the parameters of the system is known as *conductance fluctuations*. In what follows we will assume that there is no magnetic field and that spin can be ignored (that is there is no spin-orbit coupling).

A schematic of the model is shown in figure 6.8. The cavity is connected to L leads or electron waveguides. The l th lead can support N_l modes. How many modes there are in each lead is determined by the geometry of the lead. We will assume that the walls of the lead and the cavity are impenetrable, that is they present a potential barrier much greater than any electron kinetic energy. In each lead, l we have a system of coordinates such that x_l axis runs along the lead and y_l runs transverse to the lead. Each lead is of fixed width W_l . In the l th lead we then have the plane waves

$$\exp[\pm i k_n^{(l)} x_l] \chi_n(y_l)$$

where the positive sign means an ingoing wave and a negative sign means an outgoing wave. The functions $\chi_n(y_l)$ are the familiar square well energy eigenstate probability amplitudes;

$$\chi_n(y_l) = \sqrt{\frac{2}{W_l}} \sin K_n^{(l)} y_l, \quad K_n^{(l)} = \frac{n\pi}{W_l}, \quad n = 1, 2, \dots \quad (6.79)$$

where $K_n^{(l)}$ is the transverse wave number. The transverse quantisation condition means only particular solutions, labeled by n can propagate in the lead. Each allowed solution is called a *mode* or *channel*. Thus there are L leads in each of which there are some maximum number N_l of modes. Far away from the scattering region the most general form of the probability amplitude in each lead is a superposition of ingoing and outgoing amplitudes,

$$\sum_{n=1}^{N_l} \left(a_n^{(l)} \frac{1}{\sqrt{v_n^{(l)}}} e^{-i k_n^{(l)} x_l} + b_n^{(l)} \frac{1}{\sqrt{v_n^{(l)}}} e^{i k_n^{(l)} x_l} \right) \quad (6.80)$$

where

$$v_n^{(l)} = \hbar k_n^{(l)} / m \quad (6.81)$$

is the ballistic velocity of the n th mode of the l th lead. We have divided out by the square root of the velocity so that the amplitude squared of the wave function in each channel will have units of flux.

We now define an N_l dimensional vector

$$\vec{a}^{(l)} = (a_1^{(l)}, a_2^{(l)}, \dots, a_{N_l}^{(l)}) \quad (6.82)$$

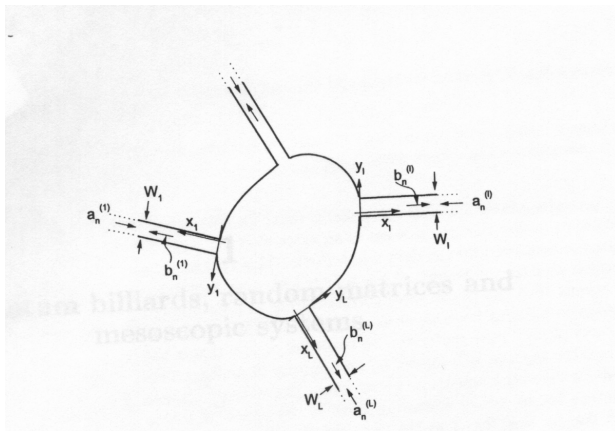


Fig. 6.8. A 2d mesoscopic cavity connected to L one dimensional leads or waveguides. The arrows indicate ingoing, $a_n^{(l)}$ or outgoing waves, $b_n^{(l)}$. In waveguide l there can be N_l such modes. (from Mello and Baranger, *Waves Random Media*, **9**, 105 (1999)).

that contains the N_l incoming amplitudes in the l th lead. We can then combine all these amplitudes for each lead in to a single vector,

$$\vec{a} = (\vec{a}^{(1)}, \vec{a}^{(2)}, \dots, \vec{a}^{(L)})^T \quad (6.83)$$

We can define a similar vector for the outgoing modes. The incoming and outgoing modes are then related by a *scattering matrix*

$$\vec{b} = S\vec{a} \quad (6.84)$$

As an example consider the case of just two leads, $L = 2$, each with N modes. Then the scattering matrix is a $2N \times 2N$ matrix and takes the form

$$s = \begin{bmatrix} r & t' \\ t & r' \end{bmatrix} \quad (6.85)$$

where r is a $N \times N$ matrix containing the reflection amplitudes for the modes of the first lead to be reflected back into the same lead, r' is for reflection from the second lead back into the second lead, t gives the transmission amplitude from modes in lead 2 to modes in lead 1, while t' gives the transmission amplitudes for modes in lead 1 into lead 2.

We now need to make a connection with the conductance. At first sight it seems strange to talk about the conductance of a system with only elastic, hamiltonian, processes. The traditional view of resistance

for normal metals treats it as due to many inelastic collisions of electrons in the Fermi sea with the ionic cores. However in mesoscopic system there are elastic collisions between the electrons and the walls of the cavity. The puzzle was solved long ago by Landauer and Buttiker. They showed that for perfectly elastic and ballistic electron transport a resistance (or conductance) could be defined in terms of the *transmission probability* for an electron to pass through the device. For example, consider a single lead so narrow that it can only support one transverse mode. Unless the reservoir connected to this lead can supply an electron with an energy that exactly matches the allowed energy of the mode in the channel, the electron will not enter the channel but will always be reflected. In that case the conductance would be zero corresponding to the zero transmission probability for the channel. As we increase the width of the channel we decrease the lowest allowed energy in the lead until it eventually falls below the Fermi energy in the reservoir. Then the transmission probability rises to unity and the conductance makes a jump from zero to a non zero value. A plot of conductance versus the width of the channel would show a series of steps as new modes open up for the reservoir to match energy. In each case the transmission probability goes from zero to unity. These conductance steps have now been observed in many experiments. The size of each conductance step is called the quantum of conductance and is given by

$$\frac{2e^2}{h}$$

a remarkable result linking fundamental constants to conductance. In the theory of Landauer and Buttiker the actual conductance of a channel of transmission probability T is

$$G = \frac{2e^2}{h} T \quad (6.86)$$

where $T = |t_{ab}|^2$ and t_{ab} is the relevant S matrix amplitude for scattering from a single mode of lead a to a single mode of lead b. In the case of multiple leads and multiple modes per channel we need to sum over initial and final modes. For the two lead case the conductance formula then becomes

$$G = \frac{2e^2}{h} \text{tr}(tt^\dagger) \quad (6.87)$$

We can simplify this by finding the eigenvalues, τ_α , of the hermitian matrix tt^\dagger

$$G = \frac{2e^2}{h} \text{tr} \sum_{\alpha} \tau_{\alpha} \quad (6.88)$$

The conductance is determined by the eigenvalues of a hermitian matrix.

To find the scattering matrix is no easy task. As we saw for the simple square well scattering problem it is ultimately determined by the allowed energy levels of the cavity responsible for the scattering. The scattering matrix is itself a unitary matrix, however it is determined by the eigenvalues and eigenvectors of the hamiltonian for the cavity. For a classically chaotic cavity these eigenvalues, or spectra, display an apparent randomness. It is at this point that we make a connection with random matrix theory. A random hamiltonian for the cavity will determine a random unitary scattering matrix. We can probe the apparently random spectra of the cavity by measuring the conductance peaks as a function of the energy of the electrons injected in to the leads from a Reservoir.

There is one final complication we need to consider. Electrons are not neutral billiard balls but carry a charge. A typical mesoscopic cavity is very small and thus has a very small capacitance, C . The energy required to put a single electron into the cavity is

$$E_c = \frac{e^2}{2C} \quad (6.89)$$

and it is likely that this will be larger than a typical spacing $\Delta E = E_n - E_{n-1}$, for the allowed energies of a neutral particle in a billiard cavity. The effect is to introduce gaps of energy E_c into the spectrum and a plot of conductance versus energy (equivalently the bias voltage) will show peaks spaced equally by the charging energy. This is called a *Coulomb blockade*. However the *height* of each peak will be determined by the scattering matrix. If there is no magnetic field we can then use the GOE random matrix theory to describe the allowed energies in the cavity which leads to an equivalent random matrix for the unitary scattering matrix S . We can then begin to model statistically the conductance peak heights using random matrix theory.

In order to find the scattering matrix we would need to find the *eigenfunctions* as well as the eigenvalues of the quasi bound states inside the dot. The reason for this is that the transmission amplitudes t_{ab} depend on the overlap of the wave function in the lead and the wave function in the dot in the vicinity of the lead. A study of the eigenfunctions of random matrix ensembles takes us beyond the scope of this subject so we will simply state the results. .

In figure 6.9 are shown the results of a model presented by Jalabert, Stone and Alhassid (Phys. Rev. Letts. **68**, 3468, (1992).) They used a GOE of random matrices to model the mesoscopic conductance of a stadium with two leads as a function of the energy of the an electron injected into one lead, but ignoring Coulomb blockade. The stadium was desymmetrised by replacing one quarter circle by a cosine curve (insert in figure 6.7). The conductance peak heights, g_n are quite variable, apparently

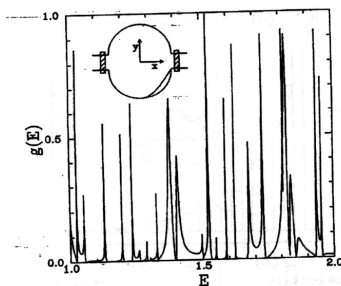


Fig. 6.9. Conductance in units of e^2/h versus energy of an injected electron for the desymmetrised stadium (from Jalabert et al. Phys. Rev. Letts. **68**, 3468 (1992)).

random.

A more detailed analysis based on random matrix theory (Alhassd and Lewenkopf, Phys. Rev. B **55**, 7749 (1997)), shows that the distribution of peak heights for a symmetric double lead chaotic mesoscopic cavity is

$$P(g) = \sqrt{\frac{1}{\pi s_0 g}} e^{-g/s_0} \quad (6.90)$$

where s_0 determines the average conductance peak height

$$\mathcal{E}(g) = \frac{s_0}{2} \quad (6.91)$$

This theory is found to be in very good agreement with experiment. In figure 6.10 are shown results for a different mesoscopic cavity of the experiment of Folk et al. Phys. Rev. Lett. **76**, 1699 (1996). Again the experiment was done for almost closed dots with two leads and no magnetic field.

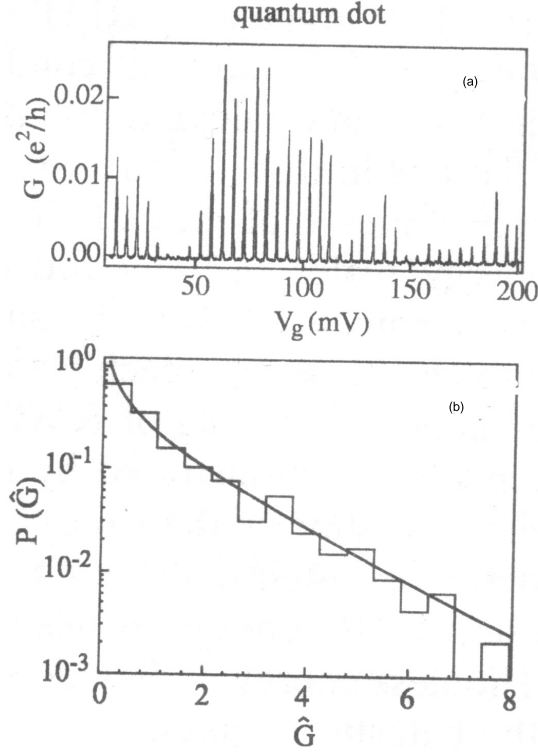


Fig. 6.10. (a) A series of Coulomb blockade conductance peaks as a function of gate voltage at zero magnetic field. (b) Distribution of the normalised conductance peak height distributions $\hat{G} = G/\bar{G}$. The solid line is the prediction of Random Matrix Theory of Jalabert et al. (from *The Statistical theory of Quantum Dots*, Y. Alhassid, Rev. Mod. Phys. **72**, 895 (2000)).

References

- [1] V.P.Maslov and N.V.Fedoriuk, *Semiclassical approximation in Quantum Mechanics*, (Redidel Dordrecht, 1981).
- [2] Gleason, A. M., Measures on the closed subspaces of a Hilbert space. J. Math. Mech. 6, 885 (1957).
- [3] U.Leonhardt and H.Paul, “Measuring the quantum state of light.”,Prog. Quant. Electr., **19**, 89 (1995).
- [4] S.L. Braunstein, C.M. Caves and G.J. Milburn, Phys. Rev. A **43**, 1153 (1991).
- [5] E. Arthurs and J.L. Kelly, Jr., Bell. Syst. Tech. J. **44**, 725 (1965).
- [6] G.J.Milburn and H.M.Wiseman, *Quantum measurement and control*, (Cambridge University Press, 2002).
- [7] R. Graham and M. Schlautman and P. Zoller, *Dynamic Localization of the Atomic Beam Deflection in a Modulated Standing Wave*, Phys. Rev. A,**45**, R19, (1992).
- [8] William H. Press and Saul A. Teukolsky and William T. Vetterling and Brian R. Flannery, *Numerical Recipes in Fortran*,(Cambridge University Press, Cambridge,New York, 1992).
- [9] Ronald D. Ruth,*A canonical integration technique*, IEE Transactions on Nuclear Science, **NS-30**, 2669, (1983).
- [10] Etienne Forest and Martin Berz, *Canonical integration and analysis of periodic maps using non-standard analysis and Lie methods*, in “Lie Methods in Optics II”,editor, Kurt Bernardo Wolf,47, (Springer-Verlag, Berlin Heidelberg,1989).
- [11] M. Abramowitz and I. A. Stegun, *Handbook of Mathematical Functions*, (U.S. GPO, Washington DC, 1965).
- [12] M. V. Berry and N. L. Balazs and M. Tabor and A. Voros, *Quantum maps*, Ann. Phys. (N.Y.),**122**,26, (1979).
- [13] E. Merzbacher, *Quantum Mechanics*, (Wiley, New York, 1970).

- [14] R. Courant and D. Hilbert, *Methods of Mathematical Physics*, vol II, (John Wiley & Sons, 1989)
- [15] C. Kittel, *Introduction to solid state physics*, (John Wiley & Sons, 1976)
- [16] C. Kittel, *Introduction to solid state physics*, (John Wiley & Sons, 1976)
- [17] J. C. Slater, *A Soluble Problem in Energy Bands*, *Phys. Rev.*, **87**, 807, (1952).
- [18] H. Risken, *The Fokker-Planck Equation*, (Springer-Verlag, Berlin, Heidelberg, New York, 1984).
- [19] , I. Sh. Averbukh and N. F. Perelman, *Fractional Revivals: Universality in the Long-Term evolution of Quantum Wavepackets Beyond the Correspondence Principle Dynamics*, *Phys. Lett.*, **139**, 449, (1989).
- [20] R. G. Littlejohn, *The semiclassical evolution of wave packets*, *Phys. Rep.*, **138**, 194, (1986).
- [21] G. M. Zaslavsky, *Stochasticity of dynamical systems*, (Nauka, Moscow, 1985).
- [22] F. Haake, *Quantum Signatures of Chaos*, (Springer-Verlag, Berlin Heidelberg, 1991).
- [23] G.P. Berman and G.M. Zaslavsky, *Theory of quantum nonlinear resonances*, *Phys. Lett. A*, **61**, 295, (1977).
- [24] G.P. Berman and G.M. Zaslavsky and A.R. Kolovsky, *On the spectrum of the system of two interacting quantum nonlinear resonances*, *Phys. Lett.*, **87**, 152, (1982).
- [25] G.P. Berman and A.R. Kolovsky, *Structure and stability of the quasi-energy spectrum of two interacting quantum nonlinear resonances*, *Phys. Lett. A*, **95**, 15, (1983).
- [26] W.A. Lin and L.E. Reichl, *Uncovering spectral repulsion in extended quasi-energy states*, *Phys. Rev. A*, **40**, 1055, (1989).